SUPPORTING INFORMATION

This supplement contains:
Supporting Materials and Methods
Supporting References
Supplementary Figure Legends
Figs. S1 to S11

Supporting Materials and Methods

Mice. P21-/- mice of mixed (C57BL/6 and 129Sv) background were obtained from Jackson laboratory and, for these studies, backcrossed in a C57BL/6J pure background (12 generations of backcrossing). C57BL/6 p53 -/- mice were obtained from Jackson Laboratory. All mouse colonies have been maintained in a certified animal facility in accordance with national and institutional guidelines.

Immunofluorescence. Cells were deposited on poly-lysine coated slides, fixed (4% paraformaldehyde), permeabilized (0.1% Triton-X), blocked (10% donkey serum), stained with different antibodies [α-p21 (SX118), Dakocytomation; α-phosphorylated (Ser139)-H2AX, Biolegend; α-phosphorylated (Ser15)-p53 and α-cleaved caspase-3, Cell Signaling; α-Ki67, BD Pharmingen] and counterstained with DAPI (Sigma) and a Cy3-, Alexa488-, or Alexa647-conjugated secondary antibody. Images were captured with a CCD (charge-coupled device) camera (Hamamatsu B/W CCD Camera CJ895), using a wide-field (Olympus BX61) or a confocal (Leica TCS SP2 AOBS) microscope. For each immunofluorescence experiment, we have analyzed 3-5 independent biological replicates and at least 50 cells/replicate.

Image Cytometry. Image Cytometry is a protocol that we have recently developed for the computer-assisted analysis of images from confocal or widefield microscopes, adapted to rare cell-populations. This protocol allows acquisition of hundreds to thousands of cell-images, through conventional automated-microscopes, and the simultaneous quantification, high-resolution localization and statistical analysis of multiple parameters, through a novel computational platform.

Briefly, cells were prepared as described in the immunufluorescence section, stained with α-cleaved caspase3, α-phosphorylated (Ser15)-p53 or α-phosphorylated (Ser139)-H2AX and counterstained with DAPI (Sigma) and a Cy3- or Alexa488-conjugated secondary antibody. Images were acquired by a robotized fluorescence microscopy station (Scan^R, Olympus); data were subsequently analyzed by an in-house developed package based on ImageJ software (W. Rasband, NIH). Number of cell analyzed for subpopulation: ~1,000 LT-HSCs, ~ 2,000 ST-HSCs, ~ 5,000 MPPs, ~ 5,000-7,000 CMPs.

Flow cytometry analysis and sorting of hematopoietic and mammary stem/progenitor cells. To analyze and isolate bone marrow LT-HSCs ($Lin^-/c\text{-}Kit^+/Sca\text{-}1^+/Flk2^-/CD34^-$) ST-HSCs ($Lin^-/c\text{-}Kit^+/Sca\text{-}1^+/Flk2^-/CD34^+$), MPPs ($Lin^-/c\text{-}Kit^+/Sca\text{-}1^+/Flk2^+/CD34^+$) and CMPs ($Lin^-/c\text{-}Kit^+/Sca\text{-}1^-$) subpopulations (2-4), bone marrow (BM) mononuclear cells (MNCs) were blocked with 10% BSA and 5% rat serum and stained with fluorochrome-conjugated antibodies against Sca1 (PE-CY5.5), c-Kit (APC), Flk-2 (PE), CD34 (FITC) or the lineage markers: Cd11b, GR1, Ter-119, IL7-R, CD3, CD4, CD8 and B220 (PE-CY7) (eBioscience). Samples were fixed with 2% formaldehyde (FA) for FACS analysis (FACSCanto, BD), or used fresh for cell sorting (FACSAria, BD) (1). To analyze and isolate mammary SCs and progenitors, primary mammary cell suspensions were stained with the PKH-26 dye (Sigma), blocked with 1% BSA, washed twice, and plated to obtain primary and secondary mammospheres. Single-cell suspensions from secondary mammospheres were sorted with a FACS Vantage SE flow cytometer (Becton & Dickinson) at a sorting pressure of 20 PSI (5).

BrdU treatment of mice. BrdU incorporation in LT-HSCs was assessed using the FITC BrdU Flow Kit (BD) (1) after two intraperitoneal injections (1 mg BrdU/mouse, every 4 hours; 4 mice/group; mice were killed 4 hours after the second injection and processed separately). In this setting, surface staining was performed as described above except for the use of a biotinylated antibody against CD34 (eBioscience), detected by APC–CY7-conjugated streptavidin (eBioscience).

Competitive Transplantation. Competitive transplantation of bone-marrow (BM) cells was performed by injecting $2x10^6$ test cells ($Ly5.2^+$) from mice irradiated 2 months before together with $5x10^5$ non-irradiated WT cells ($Ly5.1^+$), or $1x10^6$ X-ray treated p21-/- cells ($Ly5.2^+$) together with $1x10^6$ X-ray treated WT cells ($Ly5.1^+$), into lethally

irradiated C57BL/6 mice (five mice per group). Variations in SC frequency in the BM were adjusted prior to transplantation. Donor contribution was assessed in PB samples by FACS analysis of the expression of Ly5.1/Ly5.2 antigens (1), and quantified by calculating the repopulating units (RU) as = (percentage of test chimerism)×(number of competitor cells$\times 10^{-5}$)/(100 − percentage of test chimerism).

Mammosphere cultures. Mammary tissues from WT, p21-/- or p53-/- mice were mechanically and enzimatically dissociated (200 U/ml collagenase and 100 U/ml hyaluronidase) for 5 h at 37 °C. After red blood cell lysis and filtering, cells were plated onto ultralow attachment plates (Falcon) at a density of 100,000 viable cell/ml (to obtain primary mammospheres) in a stem cell medium (5 μg/ml insulin, 0.5 μg/ml hydrocortisone, 1x B27, 20 ng/ml EGF and bFGF, and 4 μg/ml heparin in MEBM medium). Mammospheres were collected after 6 days and mechanically dissociated, using a fire-polished pipette. For serial passage experiments, 5,000 cells from disaggregated primary-mammospheres were plated in 24 multiwell plates and, after 6 days, disaggregated and re-plated at the same density.

Transplantation experiments. Cells from disaggregated mammospheres were resuspended in PBS at the appropriate cell density (such that 20 μl PBS contained the correct number of cells) and injected into the cleared fat pad of the 4th mammary glands.

Q-RT-PCR. RNA expression analyses were performed using the TaqMan Cells-to-CT kit (Ambion). Three biological replicates were included for each experiment.

Intracellular localization of Numb was performed as described (5). Briefly, PKH^{high} cells were plated in the presence of 25 μM blebbistatin, a small molecule that arrests cytokinesis and leads to the formation of binucleated cells. After 36 hours, cells were fixed with 4% paraformaldehyde, permeabilized with 0.1% Triton X-100 and stained with anti-Numb followed by anti-mouse Alexa 647 (Jackson Laboratories) antibodies. Confocal analysis was performed using a Leica TCS SP2 AOBS microscope. For each cell, 15-20 adjacent 0.5 μm optical sections were collected. Each experiment was performed separately three times.

Time-lapse microscopy of the proliferative potential of PKH^{high} cells. Time-lapse microscopy of methylcellulose-plated PKH^{high} cells was performed with a Scan^R screening station (Olympus-SIS), as previously described (5). DIC (differential

interference contrast) and PKH-fluorescence images were captured every hour for 7 days, starting 14 hours after plating and immediately after irradiation. Images were collected with auto-focusing procedures and compensated for focal shift. Different focal planes were recorded to prevent loss of image contrast due to axial cell movement. Images were reconstructed using the ImageJ software.

Time-lapse microscopy of GFP expression (to assay p53-dependent transcription). Mammoshere cell suspensions from M1 were transduced with a lentivirus expressing a short half-life (<60 min) GFP under a minimal CMV promoter and 4 copies of a p53-binding site (SBI), and then plated in methylcellulose. Time-lapse microscopy was performed with a Scan^R screening station (Olympus-SIS), as described above. DIC (differential interference contrast) and GFP-fluorescence (p53 activity) images were captured every hour for 7 days, starting 14 hours after plating and immediately after irradiation. MaSCs were identified retrospectively as mammosphere-initiating cells. Fluorescence intensity per cell was measured after background subtraction using the ImageJ analysis software, and normalized to cell intensity levels at 15 hours prior to division. Each experiment was performed at least four independent times.

Supporting References

1. Viale A, *et al*. (2009) Cell-cycle restriction limits DNA damage and maintains self-renewal of leukaemia stem cells. *Nature* 457: 51-56.
2. Christensen JL & Weissman IL (2001) Flk-2 is a marker in hematopoietic stem cell differentiation: a simple method to isolate long-term stem cells. *Proc Natl Acad Sci U S A* 98: 14541-14546.
3. Osawa M, Hanada K, Hamada H, & Nakauchi H (1996) Long-term lymphohematopoietic reconstitution by a single CD34-low/negative hematopoietic stem cell. *Science* 273: 242-245.
4. Yang L, *et al*. (2005) Identification of Lin(-)Sca1(+)kit(+)CD34(+)Flt3- short-term hematopoietic stem cells capable of rapidly reconstituting and rescuing myeloablated transplant recipients. *Blood* 105: 2717-2723.
5. Cicalese A, *et al*. (2009) The tumor suppressor p53 regulates polarity of self-renewing divisions in mammary stem cells. *Cell* 138: 1083-1095.

Supporting Figure Legends

Fig. S1. Kaplan-Meier survival curves of X-ray - treated WT and p21-/- mice. WT and p21-/- mice were irradiated with different doses of X-rays and monitored for survival for one month.

Fig. S2. Image-cytometry quantification of frequency and intensity of P-p53 positive cells in untreated (Ctr) or irradiated LT-HSCs, ST-HSCs, MPPs and CMPs. For each subgroup, the negative population was identified according to P-p53 expression level frequency in the untreated sample. All intensities were then normalized to the mean fluorescence level of the defined negative region in each hystogram (red box). Some representative images are shown in the inset of the dot plot. AU: arbitrary units.

Fig. S3. A. Immunofluorescence of p21 expression in Ctr or irradiated (at 6 hrs) p53-/- LT-HSCs, ST-HSCs, MPPs and CMPs (*in vivo* experiment). For quantitation see Fig. 1E in the main text. **B.** Immunofluorescence of cleaved caspase 3 (C3) and P-p53 expression in Ctr or irradiated (at 6 hrs) p21-/- LT-HSCs, ST-HSCs, MPPs and CMPs (*in vivo* experiment). For quantitation see Fig. 2E in the main text.

Fig. S4. Q-PCR analysis of pro-apoptotic (Noxa, Puma, Bax, Bim) and pro-survival (Bcl-2, Bcl-xL) gene induction in WT or p21-/- LT-HSCs. WT and p21-/- mice were treated *in vivo* with X-rays (5.5 Gy). After 4 hrs, mice were sacrificed, LT-HSCs were purified by FACS, and RNA expression was analyzed as described (Supporting Materials and Methods section). Relative values, normalized to non-irradiated controls, are expressed as mean ±SD of triplicates.

Fig. S5. WT MaSCs are resistant to X-ray-induced apoptosis. **A.** Percentage of cleaved caspase 3 (C3)-positive cells in control (Ctr; 0 Gy) or irradiated (2, 4, 8 Gy) cell-suspensions from primary mammospheres 6 hours after treatment. **B.** Relative numbers of M2 obtained from irradiated (2, 4, 8 Gy) WT M1-mammospheres, normalized to non-irradiated controls (Ctr; 0 Gy).

Fig. S6. p21 up-regulation in MaSCs prevents X-ray-induced apoptosis. Cells from disaggregated primary WT (**A**) or p21-/- (**B**) mammospheres were infected with lentiviral vectors expressing the Green Fluorescent Protein (GFP) and, respectively: i) a p21-specific short-hairpin RNA (p21sh) or the corresponding scrambled RNA (Scramble), or

ii) p21 cDNA (p21) or nothing (mock). Secondary mammospheres obtained from infected cells were disaggregated, treated with X-rays at the indicated doses and plated to obtain tertiary (M3) and quaternary (M4) mammospheres. Infection efficiency was evaluated by immunofluorescent analysis of GFP positive cells (WT + Scramble=92.5%, WT + p21sh=94.2%, p21-/- + mock=90.8%; p21-/- + p21=92.7%. **A**. Number of spheres (±SD of quadruplicates) obtained from serial replating of Scrambled (black columns) or p21sh (white columns) infected cells, normalized to non-irradiated controls (0 Gy). **B**. Number of spheres (±SD of quadruplicates) obtained from serial replating of mock (white columns) or p21 (black columns) infected cells, normalized to non-irradiated controls (0 Gy). P values were calculated by Student's t-test.

Fig. S7. Extent of persistent DNA damage in progenitor cells. **A-B.** Percentage of γH2AX-positive cells (>4 foci/cell) in WT, p21-/- and p53-/- control (Ctr) and irradiated MPPs and CMPs, 6 hrs or 2 months after X-ray treatment of mice. **C**. Percentage of γH2AX-positive cells (>4 foci/cell) in WT and p21-/- progenitors (PKH^{low}). **D.** Percentage of γH2AX-positive cells (≥2 foci/cell) in WT or p21-/- disaggregated cells from: non-irradiated primary mammospheres (1w/M1), irradiated mammospheres, analyzed after 6 hours (+6h/M1) or 1 week (+1w/M2), primary and tertiary non-irradiated mammospheres (1w/M1 and +2w/M3). Values are expressed as mean ±SD of triplicates.

Fig. S8. Transplantation of irradiated MaSCs**. A.** Cells from WT primary mammospheres (M1) were irradiated (4 Gy) and replated to form secondary mammospheres (M2). **B-C.** Disaggregated M2 control and irradiated cells were transplanted in limiting dilution (from 100,000 to 10 cells) into cleared mammary fat pads. **B**: carmine-stained whole mount of typical outgrowths after injection of 50 cells from irradiated M2 mammospheres. **C:** Table summarizing SC frequencies (estimates with upper/lower limits) assessed by limiting dilution analysis. Fitting to the single hit model is indicated by p values > 0.05 (Fit).

Fig. S9. Analysis of division mode and p53 activation in MaSCs following X-rays. **A.** Frequencies of asymmetric and symmetric divisions of control (Ctr)and irradiated WT or p21-/- MaSCs (PKH^{high} cells), as determined by analysis of the division history of single PKH^{high} cells. PKH^{high} cells were plated in methylcellulose and observed by time-lapse. The first division was defined as "asymmetric" if one of the first-generation daughter

cells remained quiescent, whereas the other divided further, giving rise to a total of five cells by day 3. It was defined as "symmetric" when both daughter cells continued to divide, giving rise to eight cells with dim fluorescence at 3 days[23]. The pie charts show the relative frequencies of asymmetric and symmetric divisions. **B.** *In vivo* fluorescence tracking of p53 activity, independent of the modality of division. Individual (left panels) and average (right panels) best-fit lines of control or irradiated WT and p21-/- MaSCs are shown. The four average best-fit lines are plotted together in the large panel on the right. m_a, slope of the average best-fit line. P values were calculated using a two-tailed Student's t-test after evaluation of the variance.

Fig. S10. Western blot (WB) of Chk2 in p53-/- MaSCs (PKH^{high}) 6 hrs after irradiation. Vinc: vinculin. PKH labelled p53-/- mammosphere cells were disaggregated and treated with X-rays (4 Gy). 6 hrs later, PKH^{high} cells were purified by FACS and analyzed by WB for Chk2 (clone 7, Millipore).

Fig. S11. Mechanistic role of Hes1 in SC radio-resistance. **A.** Q-PCR analysis of Hes1 expression in control and X-ray treated WT or p21-/- LT-HSCs, ST-HSCs, MPPs and CMPs. WT and p21-/- mice were treated *in vivo* with X-rays (5.5 Gy). 6 hrs later, mice were sacrificed, stem/progenitor populations were purified by FACS-sorting, and RNA expression was analyzed as described (Supporting Materials and Methods section). Relative values, normalized to non-irradiated controls, are expressed as mean ±SD of triplicates. **B-C.** Cells from disaggregated primary WT mammospheres were infected with lentiviral vectors expressing a Hes1-specific short-hairpin RNA (PLKO.1- shHes1) or the corresponding scrambled RNA (Scramble), and selected with puromycin (1 μg/ml). Secondary mammospheres (M2) obtained from infected cells were disaggregated and **B**: analyzed by WB for Hes1 expression, or **C**: treated with X-rays (4 Gy) and plated to obtain tertiary (M3) and quaternary (M4) mammospheres. Numbers of spheres (±SD of quadruplicates) obtained from serial replating of mock or shHes1 infected cells, normalized to non-irradiated controls, are shown. P values were calculated by Student's t-test.

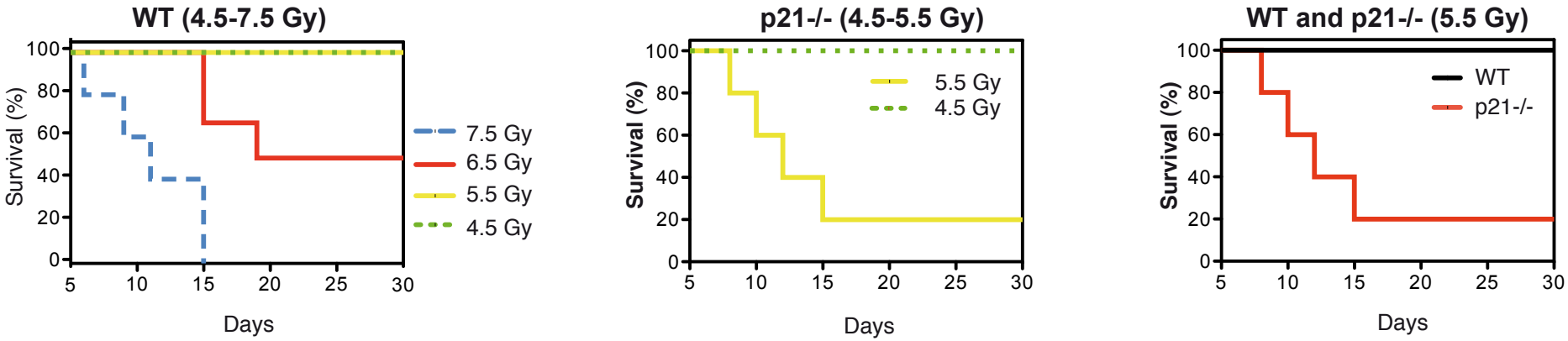
WT (4.5-7.5 Gy)
Survival (%)
100
80
60
40
20
0
5
10
15
20
25
30
Days
7.5 Gy
6.5 Gy
5.5 Gy
4.5 Gy
p21-/- (4.5-5.5 Gy)
Survival (%)
Days
5.5 Gy
4.5 Gy
WT and p21-/- (5.5 Gy)
Survival (%)
Days
WT
p21-/-

Fig. S1

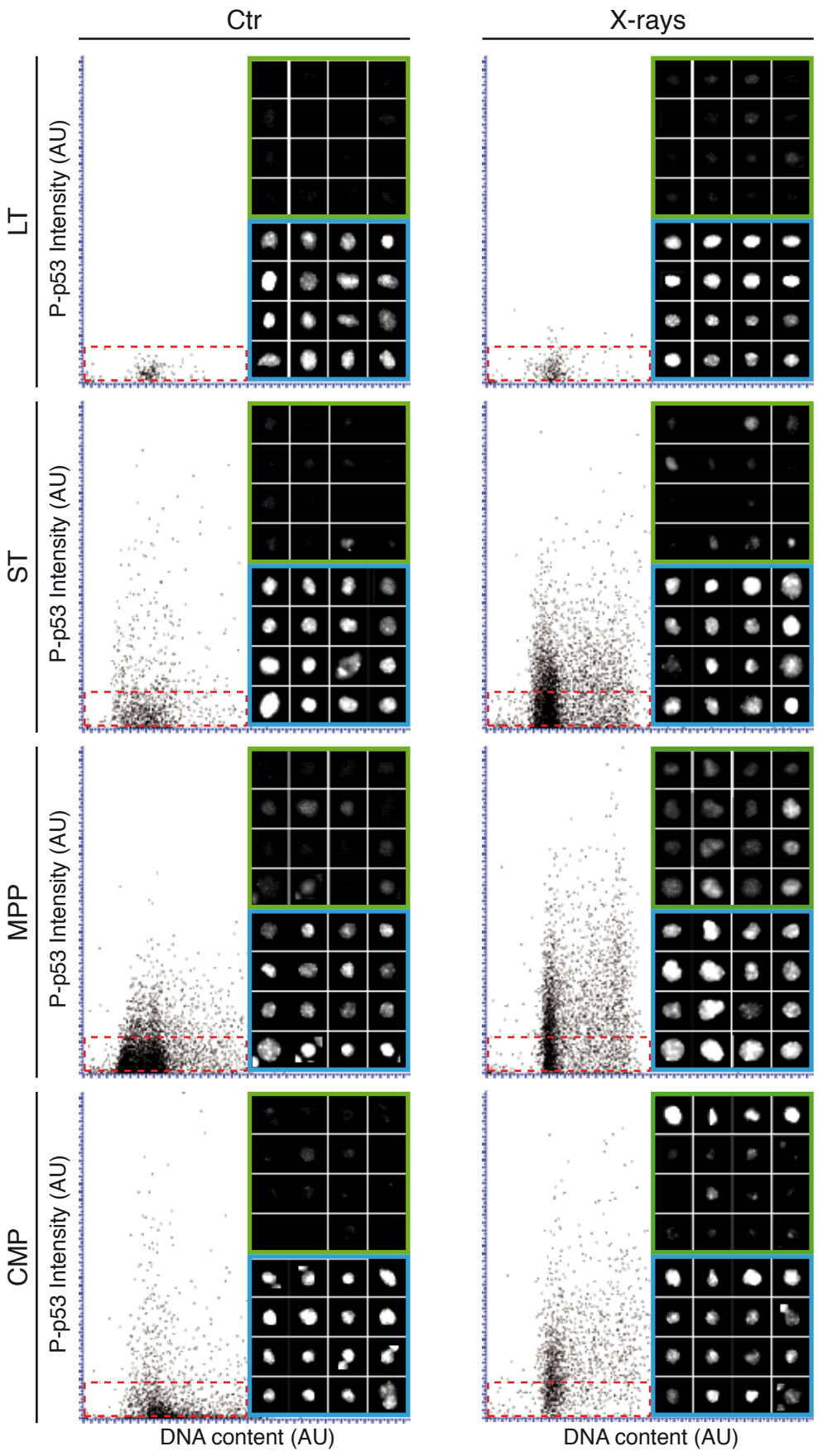

Fig. S2

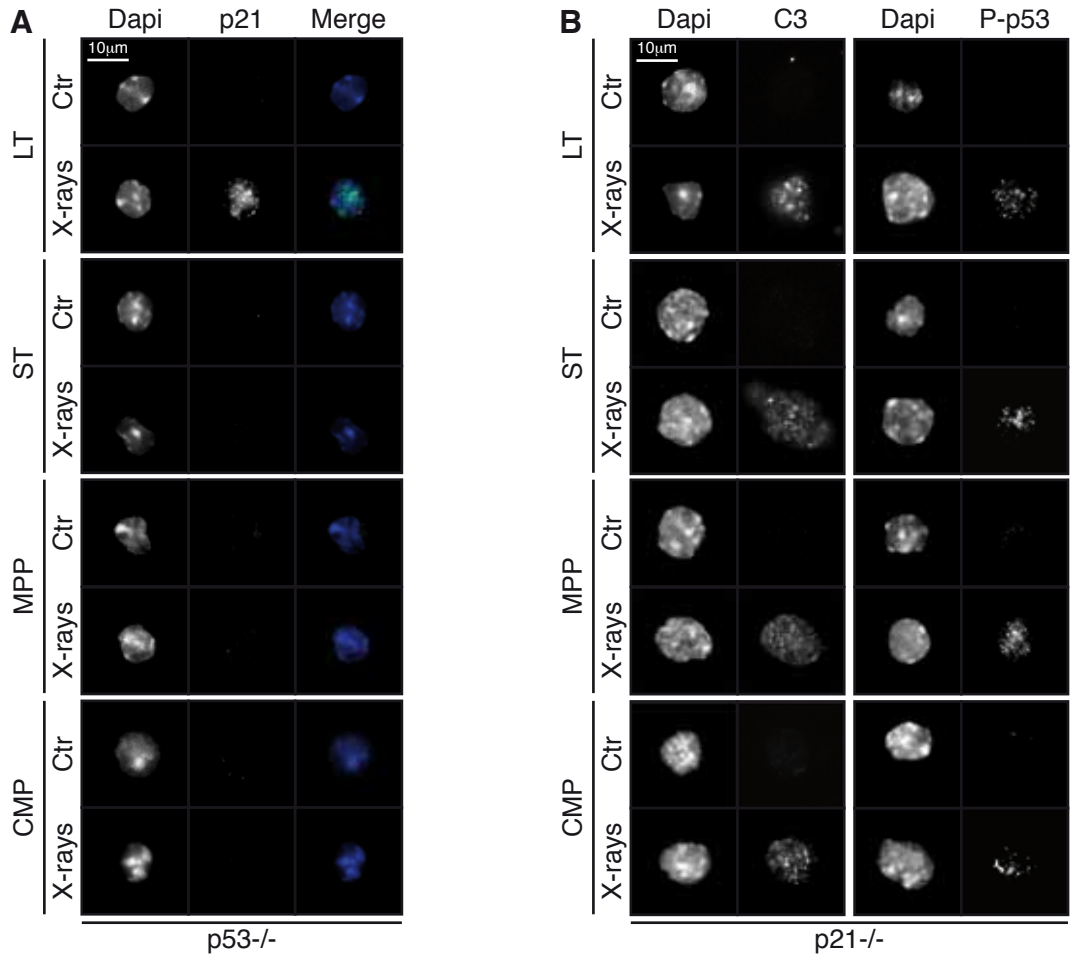
A
Dapi
p21
Merge
10μm
LT
ST
MPP
CMP
Ctr
X-rays
p53-/-
B
Dapi
C3
Dapi
P-p53
10μm
LT
ST
MPP
CMP
Ctr
X-rays
p21-/-

Fig. S3

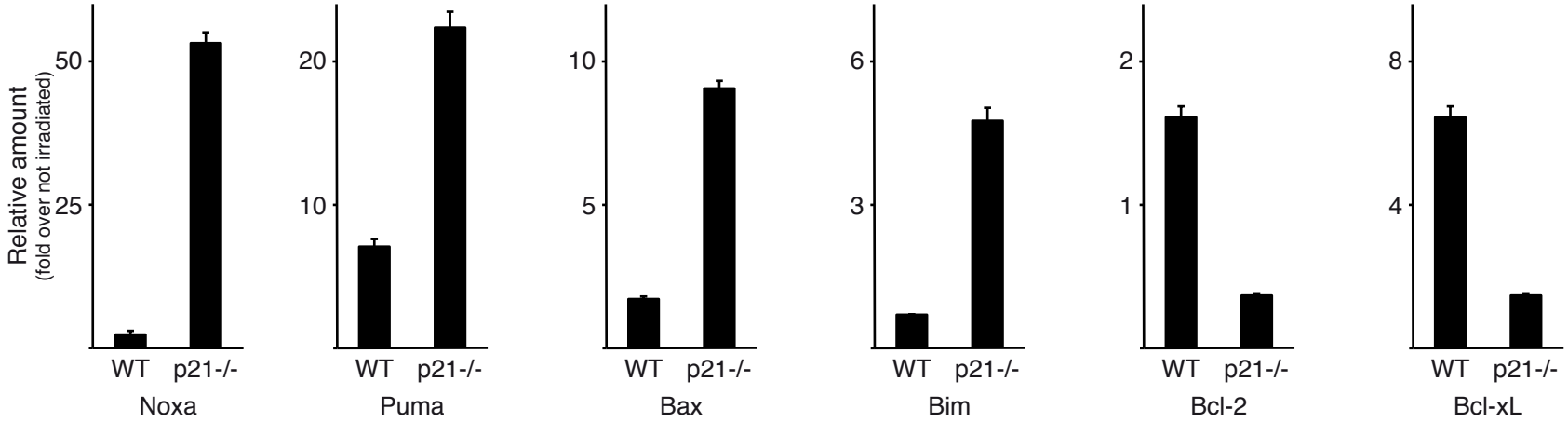
Relative amount
(fold over not irradiated)
50
25
20
10
10
5
6
3
2
1
8
4
WT
p21-/-
Noxa
Puma
Bax
Bim
Bcl-2
Bcl-xL

Fig. S4

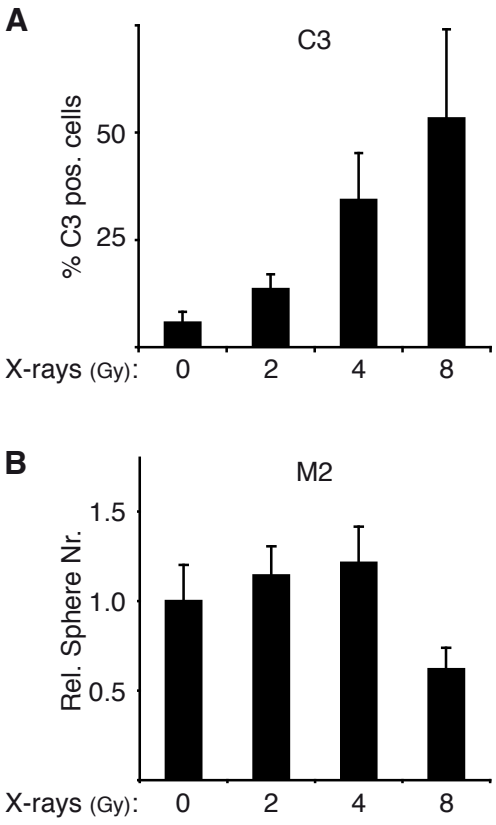
A
C3
% C3 pos. cells
50
25
X-rays (Gy):
0
2
4
8
B
M2
Rel. Sphere Nr.
1.5
1.0
0.5
X-rays (Gy):
0
2
4
8

Fig. S5

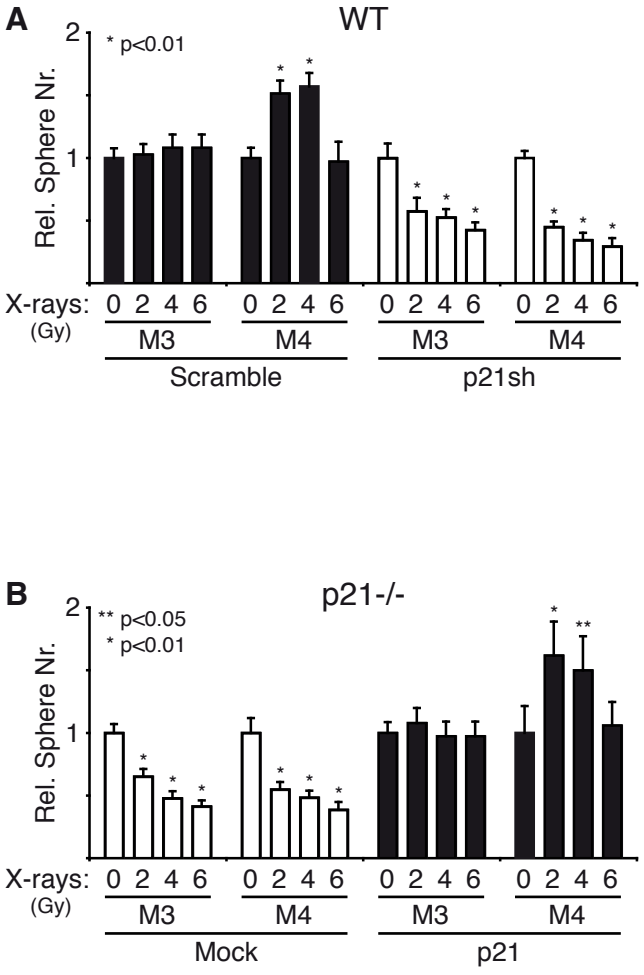
A
WT
* p<0.01
Rel. Sphere Nr.
2
1
X-rays:
(Gy)
0 2 4 6 0 2 4 6 0 2 4 6 0 2 4 6
M3
M4
M3
M4
Scramble
p21sh
B
p21-/-
** p<0.05
* p<0.01
Rel. Sphere Nr.
2
1
X-rays:
(Gy)
0 2 4 6 0 2 4 6 0 2 4 6 0 2 4 6
M3
M4
M3
M4
Mock
p21

Fig. S6

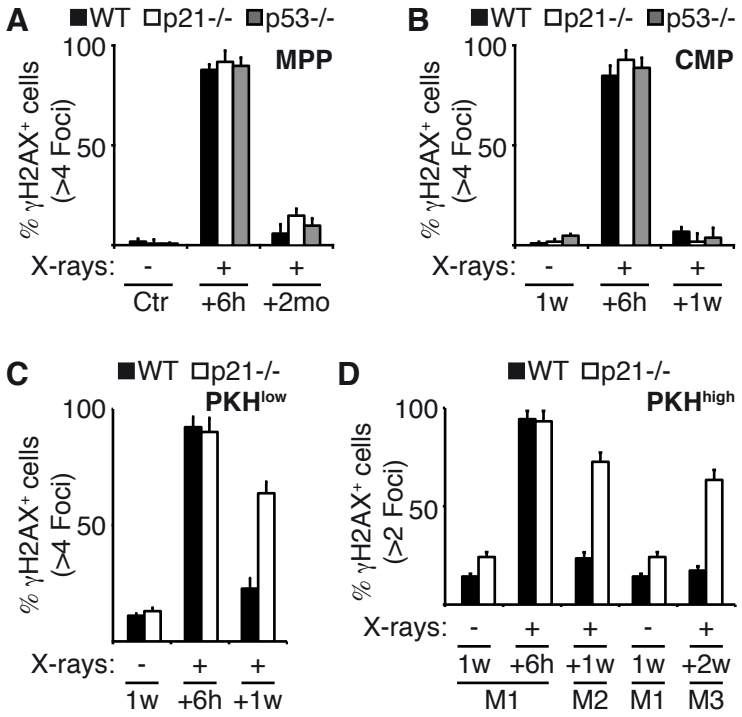
A
WT
p21-/-
p53-/-
MPP
% γH2AX+ cells (>4 Foci)
100
50
X-rays: - + +
Ctr +6h +2mo
B
WT
p21-/-
p53-/-
CMP
% γH2AX+ cells (>4 Foci)
100
50
X-rays: - + +
1w +6h +1w
C
WT
p21-/-
PKHlow
% γH2AX+ cells (>4 Foci)
100
50
X-rays: - + +
1w +6h +1w
D
WT
p21-/-
PKHhigh
% γH2AX+ cells (>2 Foci)
100
50
X-rays: - + + - +
1w +6h +1w 1w +2w
M1 M2 M1 M3

Fig. S7

A

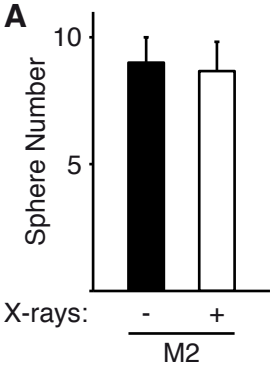

B

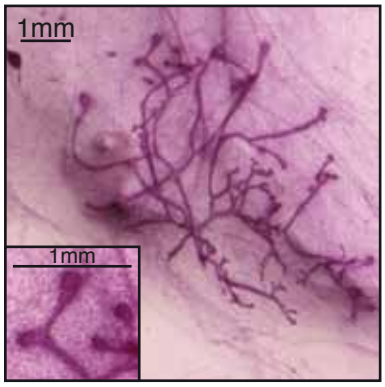

C

Cell Nr.	positive / total injections Ctr	X-rays
10^5	2/2	2/2
10^4	2/2	2/2
10^3	4/4	4/4
$5x10^2$	4/6	6/6
10^2	2/8	4/8
50	0/6	1/6
10	0/2	0/2
SC frequency (upper - lower limits)	**1:407** (1:208 - 1:797)	**1:151** (1:76 - 1:298)
p Value (Fit)	0.445	0.286
p Value (Diff.)		0.047

Fig. S8

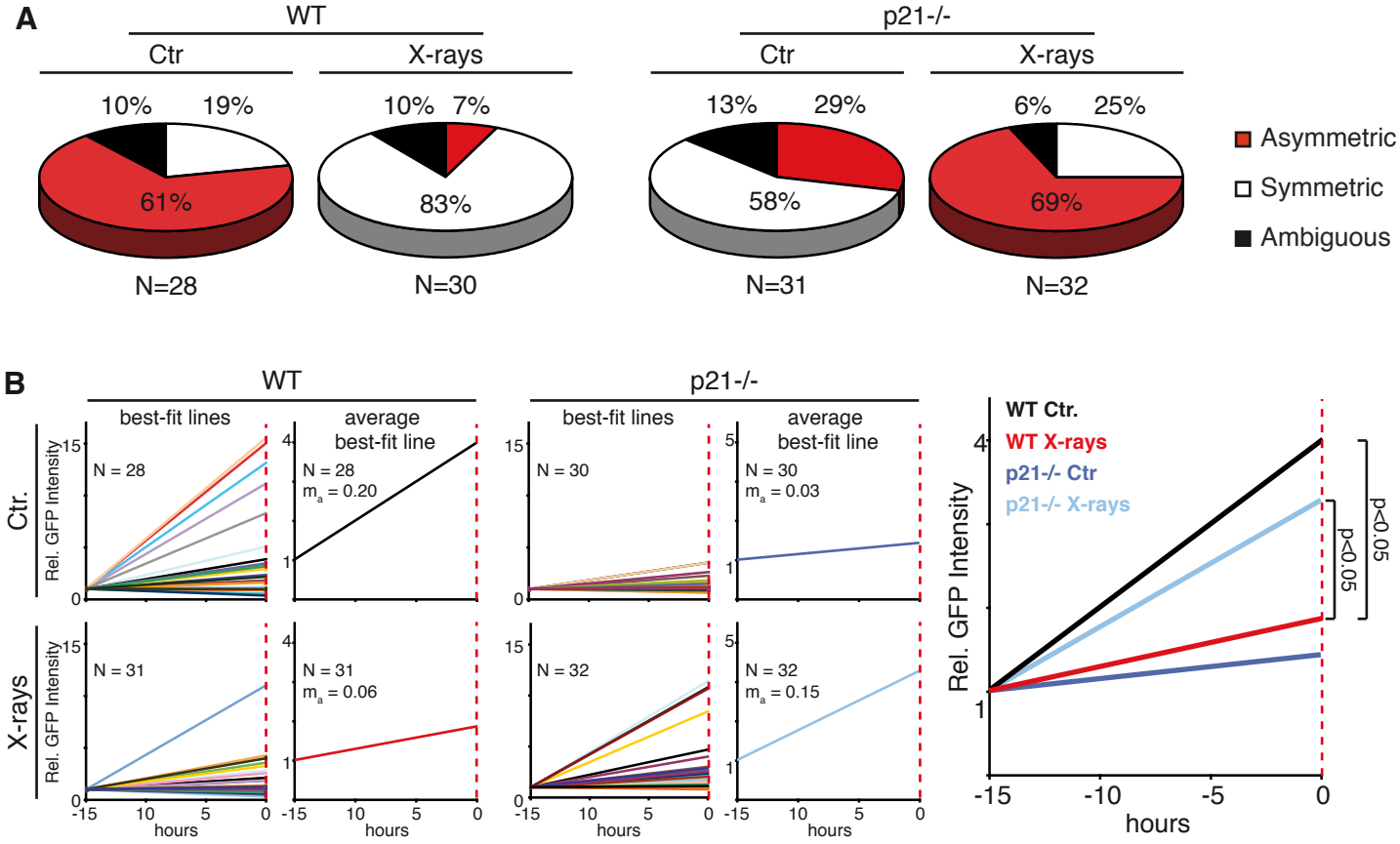
A
WT
Ctr
X-rays
p21-/-
Ctr
X-rays
10%
19%
61%
N=28
10%
7%
83%
N=30
13%
29%
58%
N=31
6%
25%
69%
N=32
Asymmetric
Symmetric
Ambiguous
B
WT
p21-/-
best-fit lines
average best-fit line
Ctr.
X-rays
Rel. GFP Intensity
N = 28
N = 28
m_a = 0.20
N = 30
N = 30
m_a = 0.03
N = 31
N = 31
m_a = 0.06
N = 32
N = 32
m_a = 0.15
hours
WT Ctr.
WT X-rays
p21-/- Ctr
p21-/- X-rays
p<0.05
p<0.05

Fig. S9

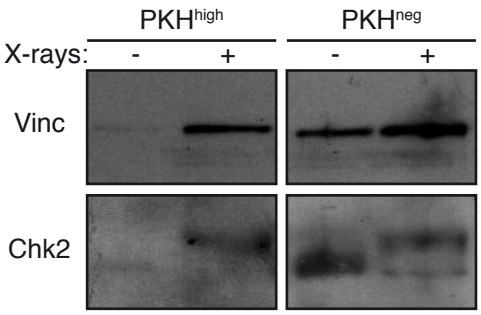

Fig. S10

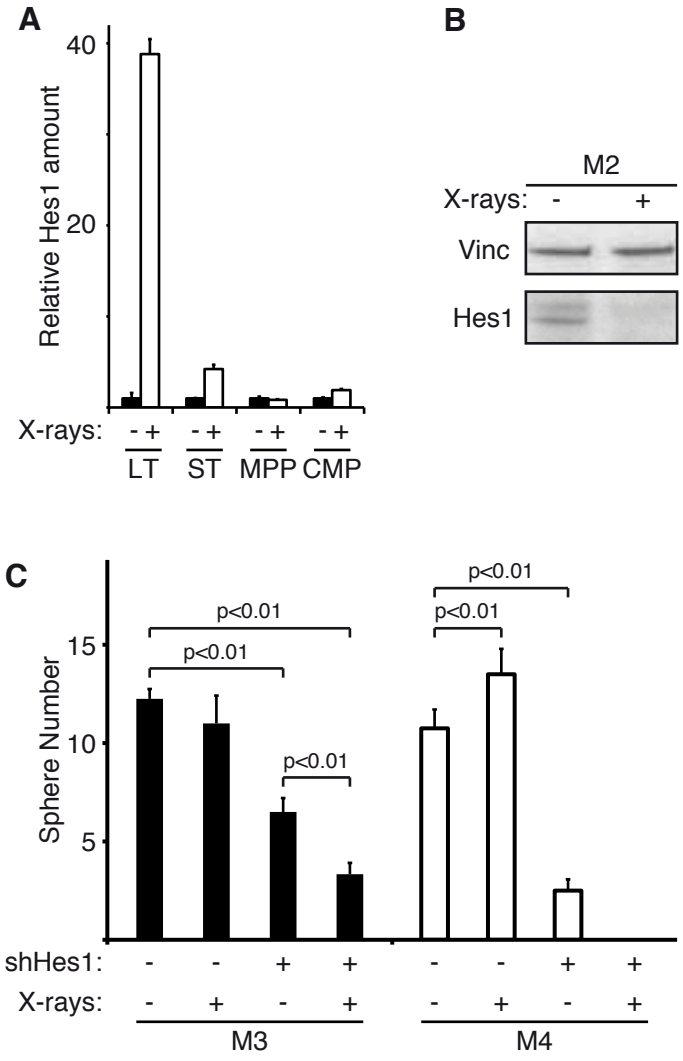
A
40
20
Relative Hes1 amount
X-rays: - + - + - + - +
LT ST MPP CMP
B
M2
X-rays: - +
Vinc
Hes1
C
p<0.01
p<0.01
p<0.01
p<0.01
p<0.01
15
10
5
Sphere Number
shHes1: - - + + - - + +
X-rays: - + - + - + - +
M3
M4

Fig. S11